

Preparation of porous Ni–Fe–Sn electrode by electrodeposition and its electrocatalytic behavior of oxygen evolution

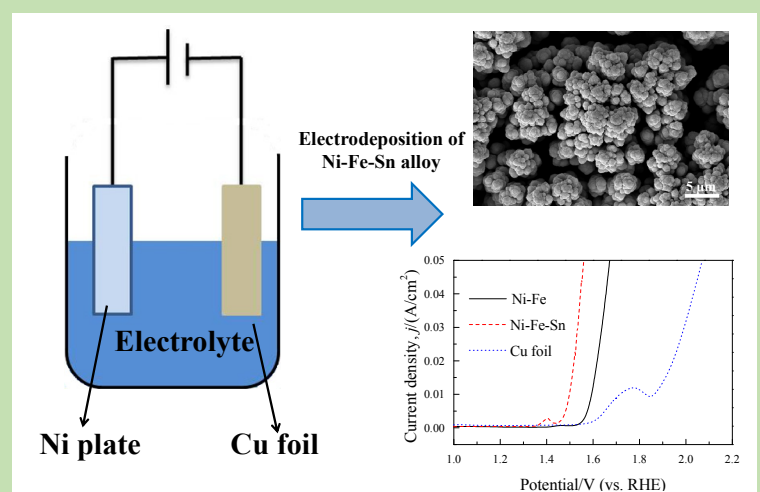
Ying GAO^{1,2*}, Yihui WU¹, Lianke ZHOU¹, Chunsheng MA¹

1. State Key Laboratory of Powder Metallurgy, Central South University, Changsha, Hunan 410083, China

2. Beijing Sinoma Synthetic Crystals Co., Ltd., Beijing 100018, China

Abstract: Oxygen evolution reaction (OER) is one of the core reactions in the field of electrochemistry and subjected to a lot of studies for many years. But it is still one of the most complicated electrochemical processes and of practical importance. Specifically, the development of efficient and low-cost non-precious catalyst for the OER is still a key challenge for the renewable energy research community. In this study, electrodeposited porous nickel–iron–tin (Ni–Fe–Sn) alloy on Cu foil as an efficient OER electrocatalyst in alkaline medium was introduced. The obtained alloy was analyzed by scanning electron microscopy (SEM) with energy dispersive spectroscopy (EDS), X-ray diffraction (XRD), respectively. The OER electrocatalytic performance of Ni–Fe–Sn alloy was investigated by linear sweep voltammetry (LSV), cyclic voltammetry (CV), electrochemical impedance spectroscopy (EIS), and chronoamperometry (CP) in 30wt% KOH solution. In addition, the Ni–Fe–Sn alloy was further tested as anodes for alkaline water electrolysis during at least 12 h with good stability. The results showed that the obtained Ni–Fe–Sn alloy was composed of Ni_3Sn_2 and FeNi_3 phases. The EDS result of Ni–Fe–Sn alloy showed the existence of three elements (Fe, Ni and Sn). SEM images displayed that the surface of the Ni–Fe–Sn alloy had porous structure, which provided more active sites for the OER. OER measurements demonstrated that the Ni–Fe–Sn alloy was highly effective for the OER with a low overpotential of 261 mV to reach $10 \text{ mA}/\text{cm}^2$ and a small Tafel slope of 69.9 mV/dec. The excellent electrocatalytic activity, long-term stability and facile preparation method enabled Ni–Fe–Sn alloy to be a viable candidate for its widespread use in various water-splitting technologies. The better OER activity of Ni–Fe–Sn alloy in comparison to Ni–Fe alloy originated from higher electrochemical active surface area (ECSA) and the improved mass/electron transport capability due to synergistic effect between Ni, Fe and Sn.

Key words: Ni–Fe–Sn alloy; oxygen evolution reaction; water splitting; electrodeposition



收稿: 2018-05-28, 修回: 2018-06-26, 网络发表: 2018-11-08, Received: 2018-05-28, Revised: 2018-06-26, Published online: 2018-11-08

基金项目: 中南大学中央高校基本科研业务费专项资金资助项目(编号: 2017zzts100)

作者简介: 高莹(1981-), 女, 山西省吕梁市人, 博士研究生, 高级工程师, 材料科学与工程专业, E-mail: gaoying0210@139.com.

引用格式: 高莹, 吴艺辉, 周连科, 等. 电沉积制备多孔 Ni–Fe–Sn 合金电极及其析氧性能. 过程工程学报, 2019, 19(1): 159–164.
Gao Y, Wu Y H, Zhou L K, et al. Preparation of porous Ni–Fe–Sn electrode by electrodeposition and its electrocatalytic behavior of oxygen evolution (in Chinese). Chin. J. Process Eng., 2019, 19(1): 159–164, DOI: 10.12034/j.issn.1009-606X.218214.

电沉积制备多孔 Ni–Fe–Sn 合金电极及其析氧性能

高 莹^{1,2*}, 吴艺辉¹, 周连科², 马春生²

1. 中南大学粉末冶金国家重点实验室, 湖南 长沙 410083

2. 北京中材人工晶体研究院有限公司, 北京 100018

摘要:采用直流电沉积法在铜箔表面合成了多孔结构的 Ni–Fe–Sn 合金, 用扫描电子显微镜、X 射线能谱仪和 X 射线衍射仪对合金的微观组织形貌和相态进行了表征, 用电化学工作站测试了合金电极在碱性环境中的析氧性能。结果表明, Ni–Fe–Sn 合金电极主要由 Ni_3Sn_2 和 FeNi_3 相组成, 电极表面形成了多孔结构。在 30wt% KOH 溶液中, Ni–Fe–Sn 合金的析氧过电位仅为 261 mV(电流密度 10 mA/cm²), Tafel 斜率为 69.9 mV/dec。电极在 10 mA/cm² 电流密度下能稳定工作 12 h 以上, 具有良好的电化学稳定性。

关键词:Ni–Fe–Sn 合金; 析氧反应; 电解水; 电沉积

中图分类号: TQ153.2

文献标识码: A

文章编号: 1009–606X(2019)01–0159–06

1 前言

氢能因具有能量密度高和清洁无污染等优点, 被视为一种理想的能源载体^[1–3]。大规模、低成本地生产氢气是开发和利用氢能的重要前提。在众多的制氢技术中, 电解水制氢具有原料来源广泛、操作简单、产品纯度高和无污染等优势, 已成为最具应用前景的制氢方法之一, 产氢量已达全球产氢量的 4%。水电解制氢过程中, 由于存在阴、阳极析氢和析氧过电位, 极大地增加了槽电压, 增加了成本^[4]。水电解过程中, 阳极析氧反应(OER)比阴极析氢反应(HER)缓慢, 其过电位比 HER 高 200~300 mV, 降低阳极的析氧过电位可一定程度上降低水电解成本^[5]。贵金属析氧催化剂(RuO_2 和 IrO_2)具有优异的析氧催化性能, 但其储量较低且价格昂贵, 难以大规模工业应用。研发廉价高效的析氧催化剂具有重要的科学意义和实际应用价值。

过渡金属(Ni, Fe 和 Co)在碱性溶液中具有较高的析氧催化活性和良好的稳定性, 在水电解工业中广泛用于阳极材料^[6]。由于 Ni 和 Fe 存在极强的协同效应, Ni–Fe 合金具有较好的 OER 活性^[7,8]。Michele 等^[9]发现掺杂锡(Sn)元素可提高 Fe_2O_3 的导电性和降低界面电荷转移电阻, 从而提高材料的析氧性能。Mani 等^[10]发现在 FeHP 中掺杂 Sn 后, 其析氧过电位由 442 mV(电流密度 $j=10 \text{ mA/cm}^2$)降到 359 mV, 原因是掺杂 Sn 提高了电子转移速度, 进而提高了材料的析氧催化活性。本工作采用直流电沉积法在铜箔表面制备 Ni–Fe–Sn 合金, 考察了合金在 30wt% KOH 溶液中的析氧催化性能, 探讨了析氧反应的动力学机理。

2 实验

2.1 材料与试剂

NaOH 、十二水磷酸三钠($\text{Na}_3\text{PO}_4 \cdot 12\text{H}_2\text{O}$)、 Na_2CO_3 、 Na_2SiO_3 、 $\text{NiSO}_4 \cdot 6\text{H}_2\text{O}$ 、 $\text{FeSO}_4 \cdot 7\text{H}_2\text{O}$ 、 $\text{SnCl}_2 \cdot 2\text{H}_2\text{O}$ 、 H_3BO_3 、 NaCl 和柠檬酸三钠($\text{Na}_3\text{C}_6\text{H}_5\text{O}_7 \cdot 6\text{H}_2\text{O}$)均为西陇化工股份有限公司产品。铜箔(广州骏丰铜铝业有限公司), 镍片(东莞市峰创金属材料有限公司)。

2.2 实验设备与分析仪器

直流稳压电源(100 V 10 A, 东莞市峰创金属材料有限公司), SHJ-2D 水浴恒温磁力搅拌器(金坛市西城新瑞仪器厂), KQ2200E 超声波清洗机(昆山市超声仪器有限公司), CHI660B 电化学工作站(上海辰华公司)。

2.3 合金电极的制备

2.3.1 基体材料预处理

以纯铜箔(纯度 99.9%, 10 mm×10 mm×0.5 mm)为阴极、大面积镍片为阳极。电沉积前用砂纸对铜箔打磨抛光, 再用热碱进行化学除油(热碱配方见表 1, 温度 70 °C, 保温时间 3 min), 用 10wt% 盐酸酸洗活化, 用去离子水冲洗干净, 烘干备用。

表 1 碱洗除油配方

Table 1 Formulation of alkaline degreasing

Agent	NaOH	$\text{Na}_3\text{PO}_4 \cdot 12\text{H}_2\text{O}$	Na_2CO_3	Na_2SiO_3
Concentration/(g/L)	15	60	25	15

2.3.2 镀液组成及工艺条件

采用单阳极单阴极体系在铜箔表面合成 Ni–Fe–Sn 合金, 镀液配方为: 100 g/L $\text{NiSO}_4 \cdot 6\text{H}_2\text{O}$, 25 g/L $\text{FeSO}_4 \cdot 7\text{H}_2\text{O}$, 10 g/L $\text{SnCl}_2 \cdot 2\text{H}_2\text{O}$, 20 g/L H_3BO_3 , 35 g/L NaCl 和 70 g/L $\text{Na}_3\text{C}_6\text{H}_5\text{O}_7 \cdot 6\text{H}_2\text{O}$, pH 值为 4.0。电沉积的电流密度为 20 mA/cm², 温度为 40 °C, 时间为

60 min。所制样品用去离子水冲洗干净，自然晾干后备用。

2.4 合金电极的物理性能和电催化性能

用ZEISS EVO18型扫描电子显微镜(SEM, 德国卡尔蔡司公司)观察Ni-Fe-Sn电极表面的微观形貌。采用XPert Powder多功能X射线衍射仪(XRD, 荷兰PANalytical公司)分析电极表面的物相组成, 管电压40 kV, 管电流30 mA, 铜靶, 波长0.15418 nm, 扫描范围 $2\theta=10^\circ\sim80^\circ$, 步长0.05°, 时间间隔1 s。

用电化学工作站对Ni-Fe-Sn合金电极进行电化学测试, 工作电极为Ni-Fe-Sn合金电极, 参比电极为饱和甘汞电极(SCE), 辅助电极为铂电极, 电解液为30wt% KOH溶液。采用线性扫描(LSV)曲线测试电极的析氧催化活性, 扫描速度2 mV/s。电化学阻抗测试(EIS)频率范围为 $10^5\sim10^{-2}$ Hz, 振幅5 mV, 测试电压为1.5 V(vs. RHE)。采用恒电流计时电位法(Chronopotentiometry, CP)在10 mA/cm²电流密度下测试其稳定性, 测试电位 E (vs. RHE)= E (vs. SCE)+0.059pH+0.197 V, 过电位 $\eta=E$ (vs. RHE)-1.23 V(理论分解电压)。

3 结果与讨论

3.1 电极表面微观结构

图1为Ni-Fe和Ni-Fe-Sn合金的XRD谱。由图可见, Ni-Fe-Sn合金中 $2\theta=43.46^\circ$, 50.52° 和 74.20° 的峰分别为FeNi₃(pdf: 38-0419)相的(111), (200)和(220)晶面, $2\theta=30.5^\circ$ 处为Ni₃Sn₂(pdf: 07-0256)相的(101)晶面。与Ni-Fe合金的XRD谱对比可知, Sn成功掺杂在Ni-Fe合金电极中。

图2为Ni-Fe-Sn合金电极的能谱, 质量比Ni:Fe:Sn=51.88:1.79:46.81, 表明Ni, Fe和Sn元素均已成功沉积进入电极中。

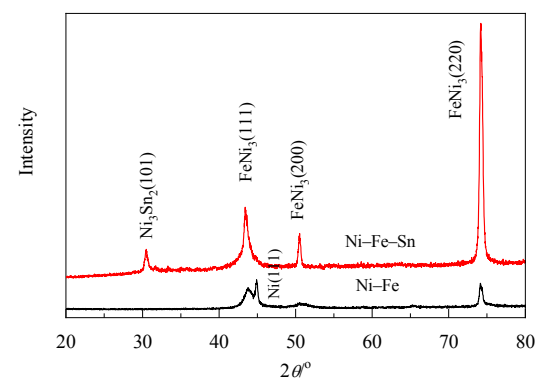


图1 Ni-Fe-Sn和Ni-Fe合金的XRD谱
Fig.1 XRD patterns of Ni-Fe-Sn and Ni-Fe alloys

图3为Ni-Fe合金和Ni-Fe-Sn合金电极的SEM照片。由图可知, 相同放大倍数下Ni-Fe合金电极的表面平整, 但存在裂纹, Ni-Fe-Sn合金电极形成了多孔结构, 原因是其具有较高的析氢催化活性, 在电沉积过程中电极表面大量析氢未及时排出, 在镀层表面大量富集形成了气泡, 破裂后导致电极表面呈多孔结构^[11,12], 可增加材料的比表面积, 有利于提高电极析氧催化性能。

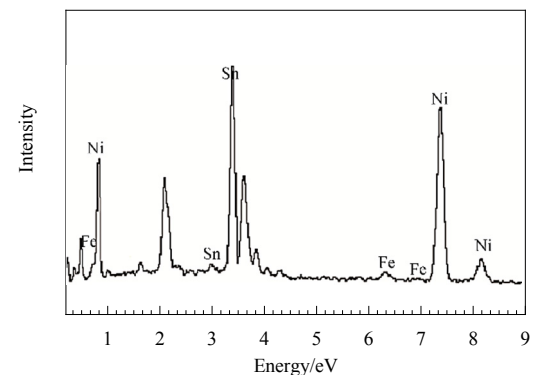


图2 Ni-Fe-Sn合金电极的能谱
Fig.2 EDS spectrum of Ni-Fe-Sn electrode

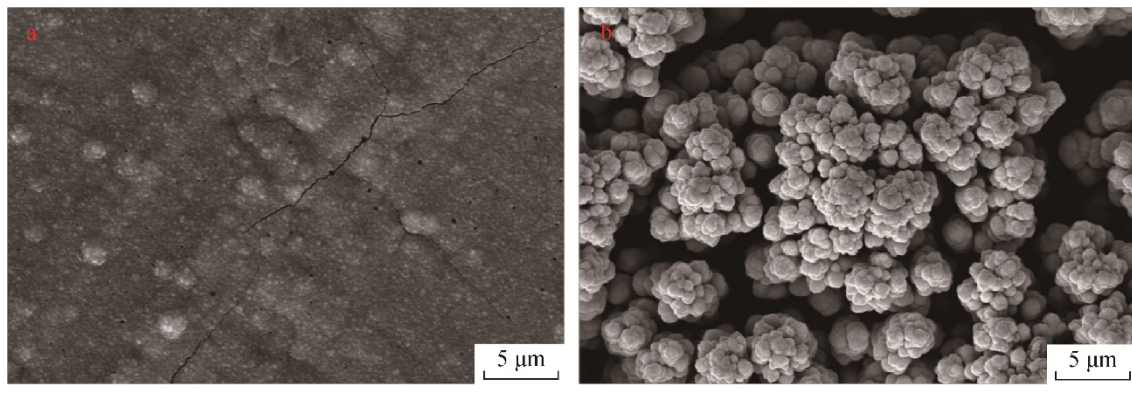


图3 Ni-Fe和Ni-Fe-Sn合金电极的SEM照片
Fig.3 SEM images of Ni-Fe and Ni-Fe-Sn electrodes

3.2 电极的电催化活性

图4为Ni-Fe-Sn和Ni-Fe合金电极作为析氧催化剂的电化学性能。由图4(a)可知,相同电压下Ni-Fe-Sn合金的电流密度比Ni-Fe合金大,表明掺杂Sn可增加Ni-Fe合金的析氧催化活性。电流密度为10 mA/cm²时,Ni-Fe-Sn和Ni-Fe合金的过电位分别为261和365 mV。为更好解释Ni-Fe-Sn和Ni-Fe合金电极的催化动

力学行为,根据Tafel公式^[13] $\eta = b \log j + a$ (其中 η 为过电势, b 为Tafel斜率, j 为电流密度)推算了Tafel斜率。一般 b 越小,反应本征动力学越快,催化性能更优。从图4(b)可知,Ni-Fe-Sn和Ni-Fe合金电极的Tafel斜率分别为69.9和89.5 mV/dec,因此Ni-Fe-Sn合金电极的本征催化动力学较快,比Ni-Fe合金的析氧催化活性高。

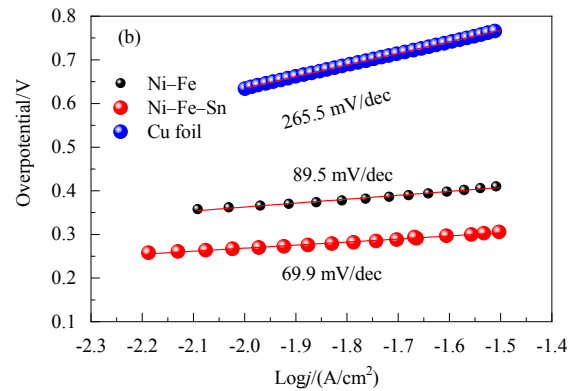
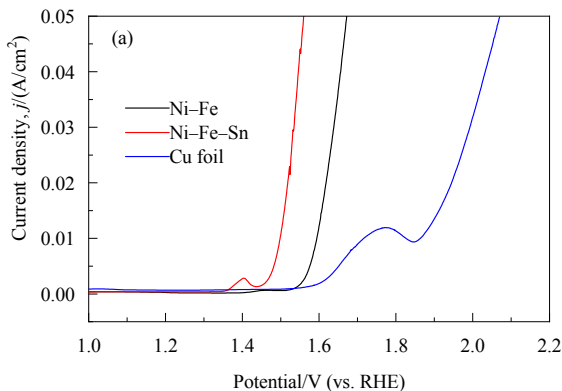


图4 Ni-Fe 和 Ni-Fe-Sn 合金在 30wt% KOH 溶液中的析氧极化曲线和相应塔菲尔曲线
Fig.4 Polarization curves of the Ni-Fe-Sn and Ni-Fe alloy electrodes in 30wt% KOH solution at 25°C and the corresponding Tafel curves of the electrodes

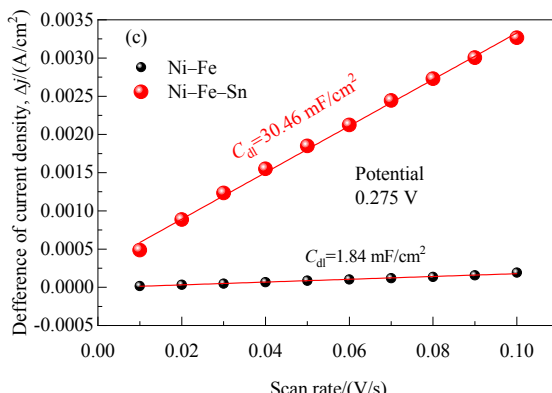
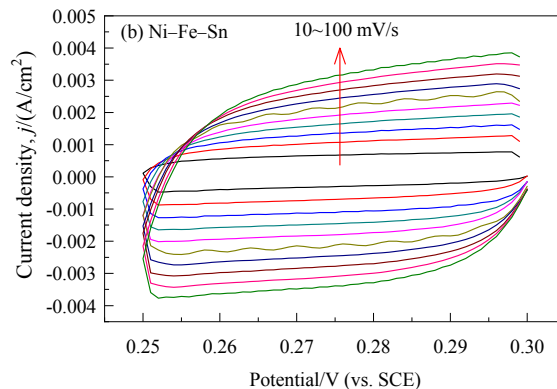
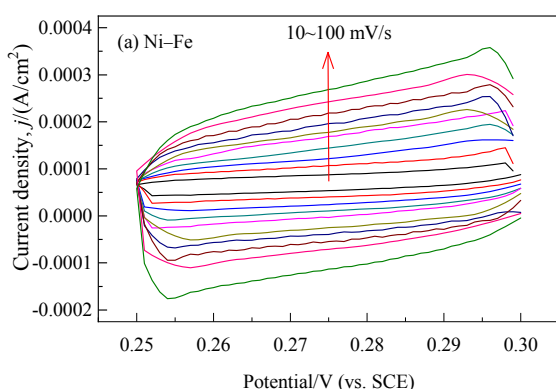


图5 不同扫面速度下合金电极的循环伏安曲线和阴极电流密度差
Fig.5 Cyclic voltammograms and difference of current density between anode and cathode of alloy electrodes under different scan rates

电极催化性能与电极比表面积有直接关系^[14,15],比表面积越大,催化活性越大,双电层电容(C_{dl})取决于电极表面积。采用循环伏安法测试电化学双电层电容,估算电极活性表面积。图5(a)和5(b)为Ni-Fe和Ni-Fe-Sn合金电极在电压0.25~0.30 V(vs. SCE)下的循环伏安曲线,扫描速率10~100 mV/s。图5(c)为合金电极的阳极电流密度(j_a)和阴极电流密度(j_c)的差值($\Delta j=j_a-j_c$)与扫描速率的关系。斜率的一半即为双电层电容(C_{dl})。由图可知,Ni-Fe-Sn和Ni-Fe电极的 C_{dl} 分别为30.46和1.84 mF/cm²。假设平滑金属表面的平均微分电容约为20 μF/cm²,则电极的活性比表面积ECSA= $C_{dl}/20$,电极的粗糙因子 $R_f=ECSA/S_{app}$, S_{app} 为电极的几何面积。电极的比表面积及相对粗糙因子如表2所示,可见Ni-Fe-Sn合金的活性表面积为Ni-Fe合金的16.5倍,与图2结果一致。

为进一步研究Ni-Fe-Sn合金电极析氧反应的动力学特征,测试了Ni-Fe和Ni-Fe-Sn合金电极在30wt%

KOH溶液中的电化学交流阻抗(EIS)谱。图6(a)为Ni-Fe和Ni-Fe-Sn合金电极在1.6 V(vs. RHE)电压下的交流阻抗。采用ZsimpWin软件拟合^[16],模拟等效电路(EEC)如图6(b)所示(R_s 为溶液电阻,反应电阻 R_{ct} 与圆弧半径有关),一般圆弧半径越大,电极上析氢电阻越大,析氢反应越不易发生。拟合参数见表3,由表可知,Ni-Fe-Sn和Ni-Fe合金电极的 R_{ct} 分别为1.06和3.97 Ω,表明Sn可使电极中的电子传输速率变快,使电极具有较高的析氢催化活性,与图4(a)的结果一致。

表2 电极的比表面积及相对粗糙因子

Table 2 The real areas and roughness factors of the electrodes

Alloy electrode	Electrochemical double-layer capacity $C_{dl}/(\text{mF/cm}^2)$	Electrochemical surface area, ECSA/cm ²	Roughness factor, R_f
Ni-Fe-Sn	30.46	1523	1523
Ni-Fe	1.84	92	92

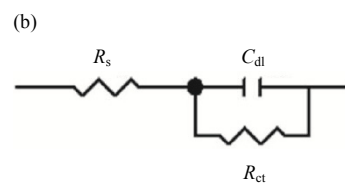
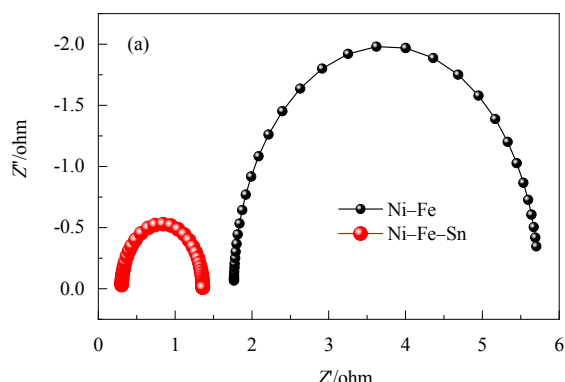


图6 Ni-Fe-Sn和Ni-Fe电极的交流阻抗和等效电路

Fig.6 Impedance spectra of Ni-Fe-Sn and Ni-Fe electrodes and electric equivalent circuit

表3 等效电路拟合的电极电化学阻抗参数

Table 3 EIS fitted parameters of the electrode equivalent circuit

Electrode	Solution resistance, $R_s/(\Omega/\text{cm}^2)$	Charge transfer resistance, $R_{ct}/(\Omega/\text{cm}^2)$	Double-layer capacity, $C_{dl}/(\text{mF/cm}^2)$
Ni-Fe	1.765	3.97	24.6
Ni-Fe-Sn	0.302	1.06	5.72

电化学稳定性是催化剂能否实际应用的主要参数之一^[17,18]。Ni-Fe-Sn合金电极的稳定性如图7所示。由图可知,在30wt% KOH溶液中,Ni-Fe-Sn电极在10 mA/cm²的电流密度下能持续工作12 h,电压基本恒定,电化学稳定性良好,具有良好的推广应用前景。Ni-Fe-Sn合金电极优异的析氧催化性能可归因于其具有多孔结构,极大地增加了比表面积,表面的活性位点增加,从而催化性能提高;Ni-Fe-Sn合金电极的导

电性好,加快了电子转移速度,从而加快了析氧反应速率。

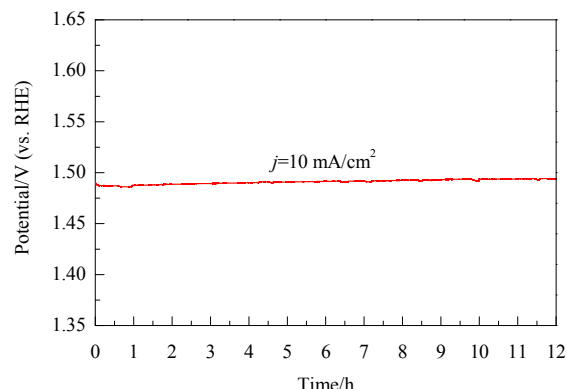


图7 Ni-Fe-Sn电极在30wt% KOH溶液中的恒电流电解曲线

Fig.7 Galvanostatic electrolysis curve of Ni-Fe-Sn electrode in 30wt% KOH solution

4 结论

采用电沉积法在铜箔表面合成了多孔的 Ni–Fe–Sn 合金电极，对合金的微观组织形貌和相态进行了表征，用电化学工作站测试了合金电极在碱性环境中的析氧性能，得到如下结论：

(1) 在 30wt% KOH 溶液中，Ni–Fe–Sn 合金电极的析氧过电位仅为 261 mV (电流密度 10 mA/cm²)，Tafel 斜率为 69.9 mV/dec。Ni–Fe–Sn 合金电极优异的析氧催化性能主要源于掺杂 Sn 后电极的比表面积增加和电子传输速率提升。

(2) 在 30wt% KOH 溶液中，Ni–Fe–Sn 电极在 10 mA/cm² 的电流密度下能持续工作 12 h，电压基本恒定，电化学稳定性良好。

参考文献

- [1] Esra T, Denizhan Ö. Fe–Cu coated nickel mesh usage as cathode catalyst for hydrogen evolution reaction [J]. International Journal of Hydrogen Energy, 2018, 43(15): 7366–7371.
- [2] Jun C, Hongmei Y. Water electrolysis based on renewable energy for hydrogen production [J]. Chinese Journal of Catalysis, 2018, 39: 390–394.
- [3] 吴靓, 郭小花, 徐阳, 等. 镍基析氢电极在碱性溶液中析氢行为 [J]. 中国有色金属学报, 2018, 28(2): 309–318.
Wu L, Guo X H, Xu Y, et al. Electrochemical performance of porous Ni-based electrodes for hydrogen evolution reaction in alkaline solution [J]. The Chinese Journal of Nonferrous Metals, 2018, 28(2): 309–318.
- [4] 冉敏, 吴艺辉, 何捍卫. 铁元素对镍基 Ni–S 合金涂层电极析氢性能的影响 [J]. 粉末冶金材料科学与工程, 2018, 23(1): 63–69.
Ran M, Wu Y H, He H W. Effect of Fe on hydrogen evolution performance of Ni-based Ni–S alloy coating electrode [J]. Materials Science and Engineering of Powder Metallurgy, 2018, 23(1): 63–69.
- [5] Wu A P, Xie Y, Ma H, et al. Integrating the active OER and HER components as the heterostructures for the efficient overall water splitting [J]. Nano Energy, 2018, 44: 353–363.
- [6] 庄林. 结晶度调控硼酸镍电催化析氧性能 [J]. 物理化学学报, 2017, 33(8): 1501–1502.
Zhuang L. Crystallinity modulates the electrocatalytic activity of nickel(II) borate for water oxidation [J]. Acta Physico-Chimica Sinica, 2017, 33(8): 1501–1502.
- [7] 何杨华, 徐金铭, 王发楠, 等. Ni–Fe 基析氧阳极材料的研究进展 [J]. 化工进展, 2016, 35(7): 2057–2062.
He Y H, Xu J M, Wang F N, et al. Recent advances in Ni–Fe-based electrocatalysts for oxygen evolution reaction [J]. Chemical Industry and Engineering Progress, 2016, 35(7): 2057–2062.
- [8] Harshad A B, Amol R J, Hern K. Facile synthesis of bicontinuous Ni₃Fe alloy for efficient electrocatalytic oxygen evolution reaction [J]. Journal of Alloys and Compounds, 2017, 726: 875–884.
- [9] Michele O, Alberto M, Giacomo A, et al. On the effect of Sn-doping in hematite anodes for oxygen evolution [J]. Electrochimica Acta, 2016, 214: 345–353.
- [10] Mani V, Anantharaj S, Soumyaranjan M, et al. Iron hydroxyphosphate and Sn-incorporated iron hydroxyphosphate: efficient and stable electrocatalysts for oxygen evolution reaction [J]. Catalysis Science & Technology, 2017, 7: 5092–5104.
- [11] 严朝雄, 王菊平, 徐志花, 等. pH 值对电沉积 NiFe 合金形貌及析氢性能的影响 [J]. 黄冈师范学院学报, 2013, 33(6): 26–29.
Yan Z X, Wang J P, Xu Z H, et al. Influence of pH on the microstructure and electrochemical hydrogen evolution of NiFe alloy [J]. Journal of Huanggang Normal University, 2013, 33(6): 26–29.
- [12] Liang J Q, Wu Y H, Zhang H A, et al. One-step electrodeposition synthesis of a Ni–Fe–Sn electrode for hydrogen production in alkaline solution [J]. Materials Letters, 2018, 227: 124–127.
- [13] 黄红菱, 于畅, 黄华伟, 等. 生物质衍生炭负载金属催化剂的制备及析氧性能研究 [J]. 新型炭材料, 2017, 32(6): 557–563.
Huang H L, Yu C, Huang H W, et al. Synthesis of biomass-derived carbon sheets decorated with metal nanoparticles and their catalytic performance in the oxygen evolution reaction [J]. New Carbon Materials, 2017, 32(6): 557–563.
- [14] Chen Z J, Kang Q, Cao G X, et al. Study of cobalt boride-derived electrocatalysts for overall water splitting [J]. International Journal of Hydrogen Energy, 2018, 43(12): 6076–6087.
- [15] Fan Q, Zhao Z H, Alam M K, et al. Trimetallic NiFeMo for overall electrochemical water splitting with a low cell voltage [J]. ACS Energy Letters, 2018, 3(3): 546–554.
- [16] 武刚, 李宁, 戴长松, 等. 阳极电沉积 Co–Ni 混合氧化物在碱性介质中的电催化析氧性能 [J]. 催化学报, 2004, 25(4): 319–325.
Wu G, Li N, Dai C S, et al. Anodically electrodeposited cobalt–nickel mixed oxide electrodes for oxygen evolution [J]. Chinese Journal of Catalysis, 2004, 25(4): 319–325.
- [17] Guan C, Xiao W, Wu H J, et al. Hollow Mo-doped CoP nanoarrays for efficient overall water splitting [J]. Nano Energy, 2018, 48: 73–80.
- [18] Fang L, Jiang Z Q, Xu H T, et al. Crystal-plane engineering of NiCo₂O₄ electrocatalysts towards efficient overall water splitting [J]. Journal of Catalysis, 2018, 357: 238–246.